Al-Manar Journal of Medical and Applied Sciences (MJMAS) 01 (1): 34-47, 2025
Doi:

Type of the Paper (Article)

Open Access

Schiff base -thiourea Mixed ligand chelates: Preparation, spectral investigation, DFT studies, anticancer activity and molecular docking

Bahya M. Al-Fakhry [1]*, Marei M.El-ajaily [2]

[1]*Chemistry Department, Faculty of Science, University of Ajdabiya, Ajdabiya, Libya*
[2]*Chemistry Department, Faculty of Science, University of Benghazi, Benghazi, Libya*

Corresponding email. *balfakry27@gmail.com*

Keywords:
Schiff base, mixed ligand chelates, thiourea, anti-cancer, DFT, molecular docking

A B S T R A C T

Here, three mixed ligand chelates of Iron(III), Cerium(IV) and thorium(IV) ions with a Schiff base resulted from coupling of L-alanine and o-hydroxyacetophenone which used as primary ligand(HL1) and thiourea as secondary ligand(L2) have been prepared and investigated by using both analytical and spectroscopic techniques. The analytical techniques showed a non-electrolytic nature character for all chelates, moreover, the chelates were formed in 1:1:1[M: L1:L2] ratio and Fe(III) mixed ligand chelates revealed a paramagnetic phenomenon, while, a diamagnetic phenomenon was observed for the Cerium(IV) and thorium(IV) ions chelates. Meanwhile, the spectral data exhibited the proper bonding between the metal ions and the activated groups present in the free ligands and the proper electronic transitions. The anticancer activity of these compounds was studied against human hepatocellular liver carcinoma (HEPG-2) cell line. The obtained results showed notable activity for all used compounds against the cell line. As per the results, the compounds were active against the cell line. The DFT calculations for these compounds were made to understand the bonding mode by a GAUSSIAN 09 program. Moreover, a docking analysis using Molecular Operating Environment (MOE) 2009.10 program was carried out against the tyrosine kinase receptor (PDBID:1M17).

Introduction

The Schiff bases are compounds that produced from the condensation of amine compounds (primary amines or amino acids) with a carbonyl (C=O) group forming new group known as imine or azomethine (C=N-) and water molecule [1,2]. This type of the compounds plays an excellent role in different range of chemistry and biology [3,4]. Thiourea compound known as thiocarbamide or sulfaurea is an organic compound of sulphur atom in its chemical structure with chemical formula $(NH_2)_2CS$. Thiourea and its complexes showed a good role in biological activity [4-7]. Halim et.al. [3] prepared and characterized a series of Cu(II)-thiourea complexes and their geometrical was square planar. Also, their antimicrobial activity was studies on some pathogenic organ species. Three mixed ligand complexes of Cr(III), Fe(III), and La(III) with 1-nitroso-2-naphthol, symbolized(NNPhH)] and amino acid L-leucine have been prepared and characterized by various physicochemical tools and an octahedral structure was proposed for all the complexes. The biological activity of all compounds has been examined against some pathogenic bacteria [8-11]. In recent years, computational chemistry has become an indispensable tool for understanding and predicting the physicochemical and biological properties of coordination compounds. Density Functional Theory (DFT) offers valuable insights into the electronic structure, charge distribution, molecular orbitals (HOMO–LUMO), and reactivity indices of metal complexes, providing a theoretical basis that complements experimental findings. Furthermore, molecular docking simulations enable the evaluation of the binding affinity and interaction mechanisms between synthesized ligands or metal chelates and biological macromolecules such as enzymes or DNA. These computational approaches contribute signifi-

cantly to elucidating the structure–activity relationship (SAR) and to rationalizing the observed antitumor and antimicrobial behaviors of coordination complexes [12-15]. Therefore, the present work integrates both experimental and theoretical investigations to achieve a deeper understanding of the structural, electronic, and biological characteristics of the prepared Schiff base–benzil mixed ligand chelates of Fe(III), Ce(IV), and Th(IV).The present study describes the formation and investigation of Schiff and mixed ligand chelates with Iron(III), Cerium(IV) and Thorium(IV) ions, in addition DFT calculations and molecular docking.

Materials and Methods

Materials

All chemicals used in this investigation were of pure grade (BDH or Aldrich). Include; L-Alanine, o-hydroxyacetophenone, thiourea, acetic acid, DMF, DMSO, NaOH, methanol, ethanol, $FeCl_3.6H_2O$, $Ce(SO_4)_2.4H_2O$, $Th(NO_3)_4.4H_2O$ and distilled water.

Measurements

The CHNS analysis for the Schiff base and mixed ligand chelates were made on 2400-CHN elemental analyzer. The molar conductivity was determined in DMF on CMD-650 digital conductivity meter. The magnetic moment measurements were done by using Gouy balance method. The infrared spectra were carried out on IFS-25 DPUS/I spectrometer. NMR spectra were recorded on Varian Gemini 200–200 MHz spectrometer using TMS as internal standard in DMSO-*d6*. The electronic and mass spectra were recorded on Perkin-Elmer lambda-365 spectrophotometer and Shimadzu QP-2010 Plus spectrometer, respectively.

Preparation of Schiff base (HL1) The amino acid Schiff base (Scheme 1) named (E)-2-((1-(2-hydroxyphenyl)ethylidene)amino)propanoic acid was prepared as follows: NaOH (0.4 g, 1 mmole) was dissolved in methanol (25 mL) and L-alanine (0.89 g, 1 mmole) was added to it. The mixture was stirred at room temperature for 5 min. When the mixture becomes homogeneous, o-hydroxyacetophenone (1.36 g, mmole) was added. After 2 min., the mixture was evaporated to 20% of its original volume and acetic acid (1 mL) was added immediately. After 2 h, a yellow product was formed, filtered off, washed, dried, and recrystallized from methanol to provide an excellent (85%) yield of pure crystals.

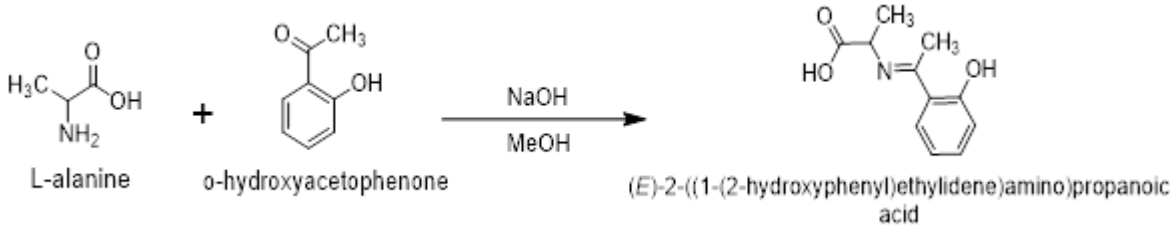

Scheme 1: Formation and structure of Schiff base

Synthesis of the mixed ligand chelates

A methanolic solution of Schiff base ligand (0.01 mole); 2.07 g was added dropsies to methanolic solution of desired metal salts, Fe(III), Ce(IV) and Th(IV) ions (1mmole;). 0.270, 0.440, and 0.552 g), respectively and the mixtures were adjusted to pH value at 8 by adding NaOH solution until the chelates formed. The mixtures were refluxed for 1.5 h, then the secondary ligand, thiourea (0.01 mole, 0.80 g) in the same amount of the solvent was added dropsies to the mixtures and refluxed for extra 3 h. The mixed ligand chelates which separated were filtrated off, then recrystallized from ethanol several times until the filtrates become clear and dried and dried in vacuum over anhydrous $CaCl_2$ [16-18].

DFT Assessment

The reported compounds were optimized and examined by Gauss View 5.0.8 graphical interface program. The DFT evaluations were carried out using GAUSSIAN09 suit programs. The very useful methods for exchange–correlation functional i.e. B3LYP is applied with 6-31 G (d, p)/LANL2DZ basic

Determination of sample cytotoxicity on cells (MTT protocol)

Cell line and culturing

The human hepatocellular liver carcinoma (HEPG-2) cell line was used for this study.

The 96 well tissue culture plate was inoculated with 1 X 105 cells / mL (100 uL / well) and incubated at 37□C for 24 h to develop a complete monolayer sheet. Growth medium was decanted from 96 well micro titer plates after confluent sheet of cells were formed, cell monolayer was washed twice with wash media. Two-fold dilutions of tested sample were made in RPMI medium with 2% serum (maintenance medium). 0.1 mL of each dilution was tested in different wells leaving 3 wells as control, receiving only maintenance medium. Plate was incubated at 37°C and examined. Cells were checked for any physical signs of toxicity, e.g. partial or complete loss of the monolayer, rounding, shrinkage, or cell granulation. MTT solution was prepared (5 mg/mL in PBS) (BIO BASIC CANADA INC). 20 uL MTT solutions were added to each well. Place on a shaking table, 150 rpm

for 5 min, to thoroughly mix the MTT into the media. Incubate (37C, 5% CO_2) for 1-5h to allow the MTT to be metabolized [19]. Dump off the media. (Dry plate on paper towels to remove residue if necessary. Re-suspend formazan (MTT metabolic product) in 200 uL DMSO. Place on a shaking table, 150 rpm for 5min, to thoroughly mix the formazan into the solvent. Read optical density at 560 nm and subtract background at 620 nm. Optical density should be directly correlated with cell quantity [20-23].

Molecular docking studies

Molecular Operating Environment (MOE) 2009.10 program was used in molecular docking studies. Docking studies were done to assess the binding free energy of the inhibitor inside the macromolecule. The Dock scoring in MOE software was done utilizing London dG scoring function and the Force-filed have been improved to check that refined poses meet the specified conformations. Auto rotatable bonds were allowed; the best ten binding poses were directed to analyze for achieving the best score. To compare the docking poses to the ligand in the co-crystallized structure and to obtain RMSD of the docking pose database browser was used [24-27].

Preparation of compounds and target EGFR tyrosine kinase receptor.

The compounds contributed in this study as ligands was studied for their binding affinity into tyrosine kinase receptor (EGFR). To build a three-dimensional model of the structures, molecular builder tool in MOE was used. Energy minimization was carried out through Force-Filed MMFF94X. Optimization was carried out using gradient of 0.001 for determining the lowest energy confirmation with most favorable geometry. The crystal structure of c-kit receptor protein-tyrosine kinase in complex were picked up from the Protein Date Bank (PDB) (PDB code: 1M17). Partial charges and hydrogen atom were put on to the protein with the protonation 3d application in MOE [28].

RESULTS

The CHNS elemental analysis data of the Schiff base and mixed ligand chelates are in good constituent with the calculated values (Table 1), this illustrates the formation of the Schiff base and mixed ligand chelates. Whereas, the molar conductance values of the mixed ligand chelates under investigation in DMF solvent (10^3 M) reveal the existence of non-electrolyte in nature, indicating that there is no anions outside the coordination sphere [29-33].

Table 1: Micro chemical analyses and some physical data of Schiff base and mixed ligand chelates

Compounds	M. wt	Color	Microchemical analyses Calcd. **Experimental**				**^m; Ω^{-1} cm^2mol^{-1}**	**μ B.M**
			C%	**H%**	**N%**	**S%**		
HL1; ($C_{11}H_{13}NO_3$)	207	Daffodil	63.77 **64.20**	6.28 **5.21**	6.76 **6.25**	----	_____	-------
[Fe((L1)(L2)(OH)].H_2O	372	Penny	38.71 **39.27**	5.38 **5.12**	11.29 **12.00**	8.60 **9.00**	0.001073	5.97
Ce (L1)(L2)(SO_4)(H_2O)].H_2O	553	Simply white	26.04 **26.75**	3.79 **3.00**	7.59 **8.01**	11.57 **11.72**	0.001255	0.00
[Th(L1)(L2)(NO_3)$_2$]2H_2O	674	Banana	21.36 **21.07**	3.12 **2.85**	6.23 **6.73**	4.75 **5.97**	0.000775	0.00

Infrared spectra

The IR spectral results of Schiff base compound (HL1) and mixed ligand chelates are listed in Table 2 and their spectra are shown in figure 1. In the spectra of the Schiff base, the strong broad band appeared at 344 cm^{-1} is due to O-H vibration of the phenolic [34]. This band vanished due to complexation with metal ion. The same spectrum shows a band at 1605 cm-1 corresponding to the formation of azomethine group (C=N) [35]. The same spectrum also exhibits a band at 3094 cm^{-1} assigned to COOH vibration [11]. The infrared spectra of the Fe(III), Ce(IV) and Th(IV) mixed ligand chelates (Table 2) and compared with free ligands to provide some details on the bonding in the chelates. In addition, the band in IR spectrum of the Schiff base at 1605 cm^{-1} is observed to be changed in the spectra of the mixed ligand chelates, confirming the donation of the lone pair of electrons on azomethine nitrogen to metal center [36]. The absence of a broad band in the 3441 cm^{-1} regions, which is observed in the spectra of the mixed ligand chelates is an indication of deprotonation of the intramolecular hydrogen bonded OH group on chelation and subsequent coordination of the phenolic oxygen to the metal ion [37]. IR spectrum of Schiff base shows a band at 3094 cm^{-1} regions assigned to COOH group of L-

alanine which is absent in the spectra of the mixed ligand chelates suggesting its participation in chelation with metal ions [38]. Moreover, the new bands in the infrared spectra of the mixed ligand chelates which are not observed in the free ligands appeared in the range of 671-601 and 583-478 cm^{-1} represented (M-O) and (M-N) vibrations indicating participation of nitrogen atom of azomethine and oxygen atoms of hydroxyl and carboxyl groups in coordination with the metal ions under investigation [39]. In IR spectra of Ce(IV) mixed ligand chelate, the bands at 1528 and 1065 cm^{-1} are due the presence of bidentate coordinate sulphate [16]. Meanwhile, in the spectrum of Th(IV) mixed ligand chelate, the bands in the range of 732-1566 cm^{-1} are signals to the spilt bands of nitrate group [40]. The band related to $–NH_2$ group is overlapped with the bands of crystal water molecules present in the mixed ligand chelates. In the infrared spectrum of Ce(IV) mixed ligand chelate, the band observed at 800cm^{-1} is attributed to the coordinate water molecule [18]. The IR spectra of the mixed ligand chelates reveal bands in the range of 868-848 cm^{-1} that have been attributed to (C=S) vibration which is not changed on chelation [41].

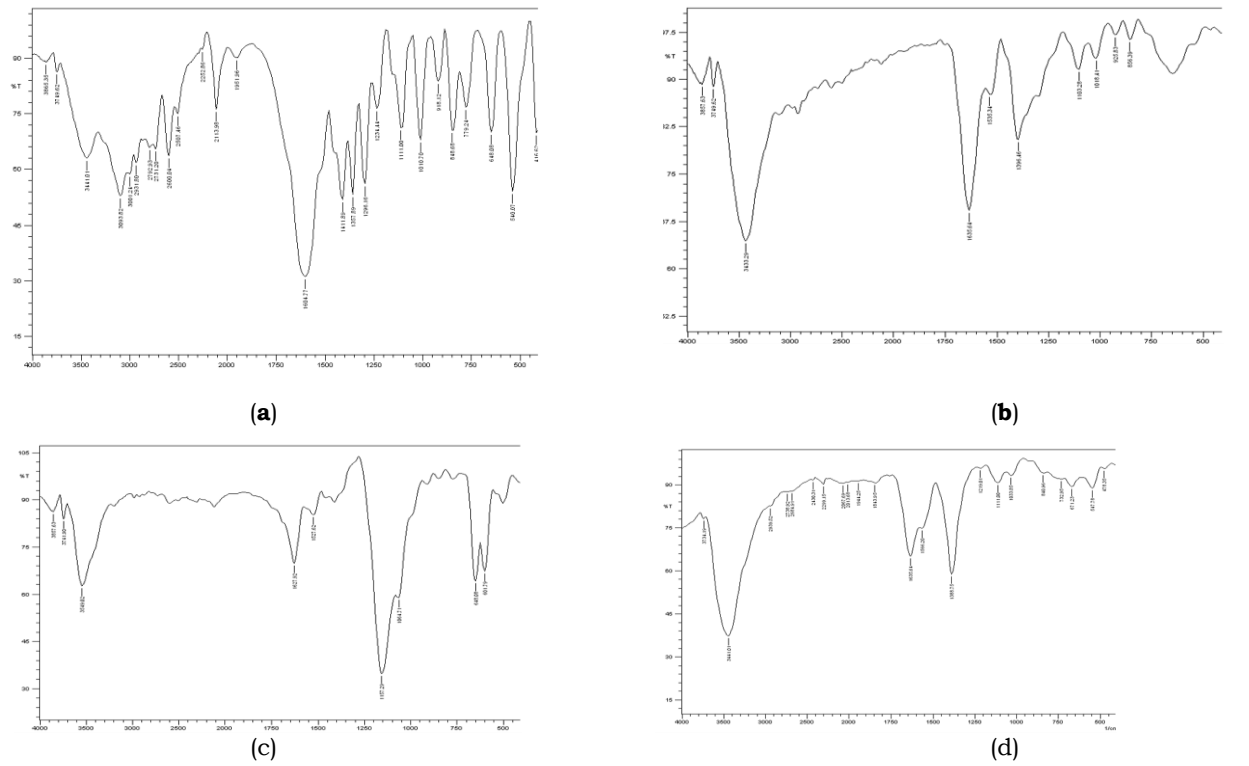

Fig. 1. Infrared spectra of (a) Schiff base (HL1), (b) $[Fe(L1)(L2)(OH)]\cdot H_2O$ mixed ligand chelate, (c) $[Ce(L1)(L2)(SO_4)(H_2O)]\cdot H_2O$ mixed ligand chelate, and (d) $[Th(L1)(L2)(NO_3)_2]\cdot 2H_2O$ mixed ligand chelate.

Table 2: Infrared spectral results(cm^{-1}) of the Schiff base and mixed ligand chelates

Compounds	**υ (OH) υ (H_2O)**	**υ (C=N)**	**υ (M-O)**	**υ (M-N)**
HL1; ($C_{11}H_{13}NO_3$)	3441	1605	---	---
$[Fe(L1)(L2)(OH)].H_2O$	3441	1636	648	531
$[Ce(L1)(L2)(SO_4)(H_2O)].H_2O$	3549	1628	640	583-601
$[Th(L1)(L2)(NO_3)_2].2H_2O$	3441	1636	671	476-548

^{1}H- and ^{13}C-NMR spectra of Schiff base

The 1H-NMR spectrum of the Schiff base was obtained in DMSO-*d6* solution as a solvent at room temperature using TMS as an internal reference. In the present study, the ^{1}H-NMR spectral signals are depicted in Fig. 2a. The resonance of protons has been assigned on the basis of their integration and multiplicity pattern. The 1H-NMR spectrum of Schiff base shows two signals at 4.1 and 7.73 ppm, the first signal attributed to presence of -OH proton in phenyl ring and -COOH group in amino acid, also the signals at 1.2, 2.3, 3.2 and 2.5 ppm are due to the existence of methyl groups and DMSO solvent, respectively [20]. The aromatic protons have been resonated in the region at 6.4-7.5 ppm [21]. ^{13}C-NMR spectrum of the Schiff base has been recorded in DMSO-d6 as a solvent. Fig. 6 exhibits a chemical shift at 170.82 ppm refers to imine carbon atom (C=N) group [22]. While the chemical shift at 173.19 ppm is attributed to the carboxylic carbon atom COOH group [23] and signals at 57.62, 19.94, and 14.23 ppm assigned to carbons of methyl groups [24]. Signals that are associated with the aromatic carbons have been detected at a range of 113.02-133.40 ppm and signal at 169. 96 ppm may be due to carbon of C-OH phenolic group [25]. The signal observed at 39.50 ppm leads to DMSO-*d6* [42].

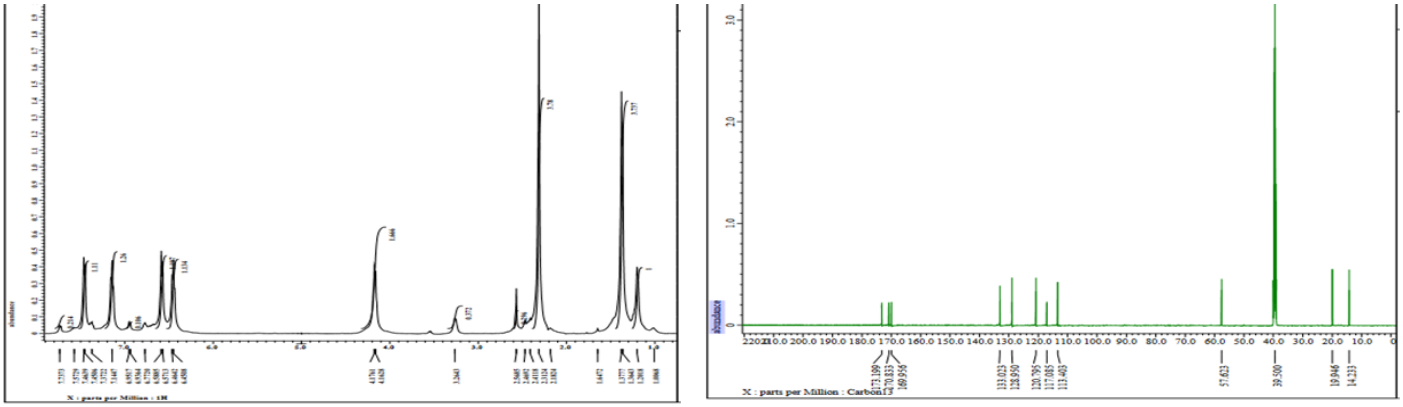

(**a**) (**b**)

Fig. 2. NMR spectra of Schiff base (HL1): (a) ^{1}H-NMR spectrum and (b) ^{13}C-NMR spectrum.

Mass spectrum of Schiff base

Fig. 3 offers the mass spectral fragmentations of the free Schiff base (HL1)
As shown below:
$C_{11}H_{13}NO_3$; m/e+= 207, $C_{11}H_{10}NO_2$; m/e+ =188, $C_8H_9NO_2$; m/e+= 151
C_7H_9O; m/e+= 109; C_7H_7; m/e+= 91

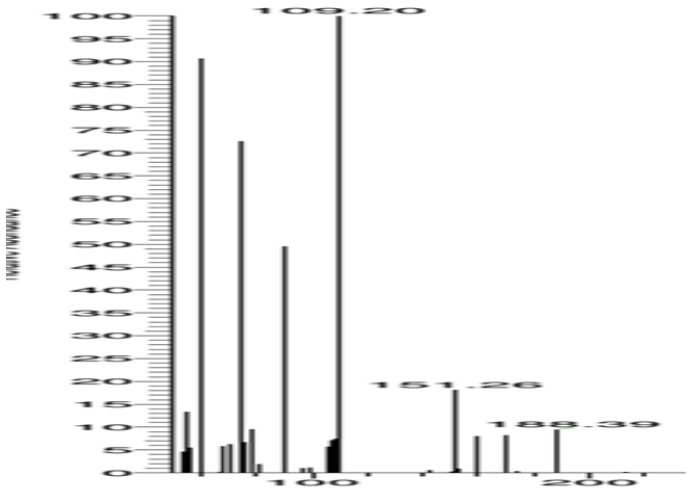

Fig.3: Mass spectrum of the Schiff base (HL1)

Electronic spectra and magnetic moment

The electronic spectral data of the Schiff base and mixed ligand chelates are listed in table-3 and their spectra are shown in Fig. 4. The spectrum of the Schiff base (HL1) exhibits absorption bands at 260 nm (38711cm^{-1}) and 313 nm (31949 cm^{-1}) corresponding to $\pi \rightarrow \pi^*$ (phenyl ring) and $n \rightarrow \pi^*$ transition, respectively [42]. The spectral data of Fe(III) mixed ligand chelate show a band at 323nm(30960 cm-1) assigned to the charge transfer transition [28]. Fe(III) complex exhibits a magnetic moment value of 5.97 B.M. at room temperature. indicating that the chelate has a high spin octahedral configuration [29]. The electronic spectra of the Ce(IV) and Th(IV) mixed ligand chelates were recorded in the UV-visible region and show bands in the range of 258-302 nm (38760-28089 cm-1), 262-298 nm (38168-33557 cm-1) and 335 nm (2985 cm-1) ascribed to $\pi \rightarrow \pi^*$ (aromatic ring) and to $n \rightarrow \pi^*$ (azomethine chromophores) respectively, The shift of the reflection bands to lower values (hypsochromic shift) and to higher values (bathochromic shift) in comparison to Schiff base ligand and appearance of new bands in the absorption spectra of the chelates, indicate that their metal chelates are forming[30]. Due to the f-f bands are line or sharp, the spectra of Ce(IV) and Th(IV) mixed ligand chelates show no obvious transitions in the region of 500-700 nm (20000-14286 cm^{-1}). This is owing to the f-orbitals being shielded by 6s, 6p or 7s, 7p orbitals [43].

Table 3: Electronic spectra (of the Schiff base and mixed ligand chelates

Compounds	λ **nm** (cm^{-1})	**assignment**
HL1; ($C_{11}H_{13}NO_3$)	**260nm**(38711cm^{-1})	$\pi \rightarrow \pi^*$,
	313 nm (31949 cm^{-1}	$n \rightarrow \pi^*$
[Fe(L1)(L2)(OH)].H_2O	**323**(32154cm^{-1})	C.T
	356nm(28089cm^{-1})	C.T
[Ce(L1)(L2)(SO_4)(H_2O)].H_2O	**258nm** (38760 cm^{-1})	$\pi \rightarrow \pi^*$
	302nm (28089cm^{-1})	$n \rightarrow \pi^*$
	500-700 nm(16667-14286cm^{-1})	f-f transitions
[Th(L1)(L2)(NO_3)$_2$].2H_2O	**262-298nm**(38168-33557cm^{-1}),	$\pi \rightarrow \pi^*$
	335nm(29851cm^{-1})	$n \rightarrow \pi^*$
	500-700 nm(16667-14286cm^{-1})	f-f transitions

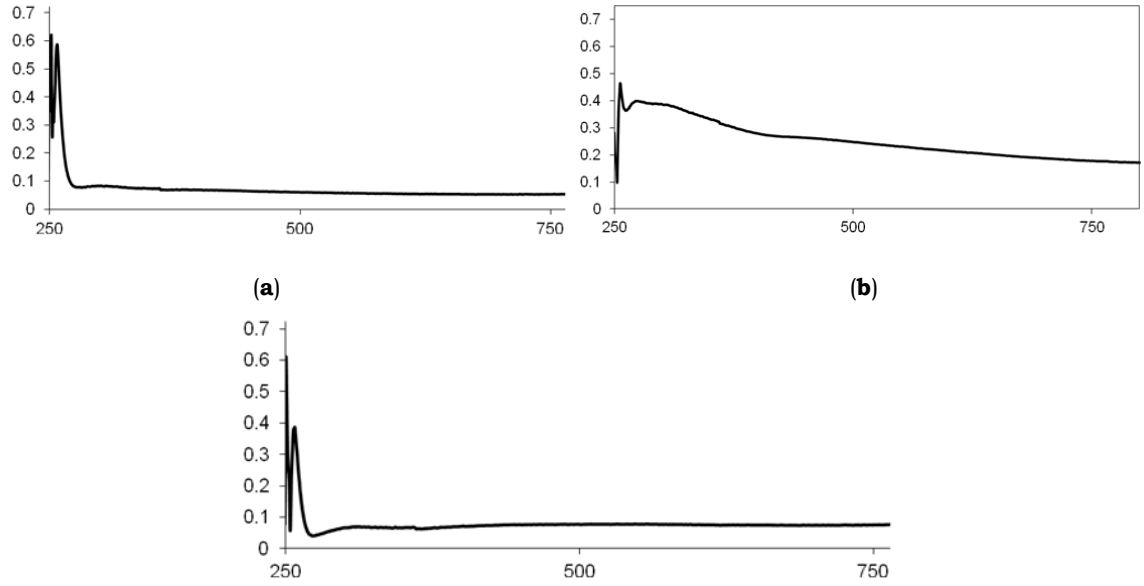

Figure 4. This is a figure. Schemes follow another format. If there are multiple panels, they should be listed as: (a) Description of what is contained in the first panel; (b) Description of what is contained in the second panel. Figures should be placed in the main text near to the first time they are cited.

DFT calculations

In the present study, GaussView 5.0.8(Wallingford, CT 2009) [32] is used to prepare the input files of compounds. All calculations were performed using Gaussian 09 rev. A.02 (Wallingford, CT, 2009) [33] by the DFT/B3LYP method. 6-311G and LANL2DZ are the standard basis sets for the synthesized ligand and its mixed ligand chelates, respectively. MOE 2009 (Molecular Operating Environment) software was used to simulate the topoisomerase IIa. The protein crystal structure of the protein with topoisomerase II DNA gyrase enzymes (antimicrobial activity) (PDB ID: 2XCT). The optimized structures of the metal chelates are shown in Fig.12 with salient metal-ligand bonds labeled in Ångstrom. Results showed the presence of H-bonds in some of the synthesized compounds and depicted as “dashed bonds” in the structures. The H-bonds in ligand and Ce-chelate forming hexa-cyclic rings. This has the tendency of enhancing the stability of our compounds. Following some observations based on the computed bond lengths, bond angle and orientations (structures) aimed at compounds (Table 4). In mixed ligand chelates, some bond lengths in ligand (HL1) were increased as [(C2-C8), (N9-C10)& (C10-C11) and others were decreased as [(C1-O7) & (C8-N9)] to adjust the coordination via the N9,O7and O14 in all mixed ligand chelates with the formation of new (N9-M), (O7-M) and (O14-M) bonds. (L) bond angles are altered by coordination as pointed out in Table 4, when the metal center is changed, large changes in the angles surrounding the metal emerge. The high change in angles values that increased or decreased as a result of bonding during chelate creation. The negative charge of the (HL) ligand is delocalized over N9,O7 and O14 with calculated charges -0.707, -0.710 and -0.567, respectively. The charge transfer from the examined (HL) ligand donor sites to the central metal ions i.e. L→M can be supported with decreasing in the calculated charges on metal ions after coordination.

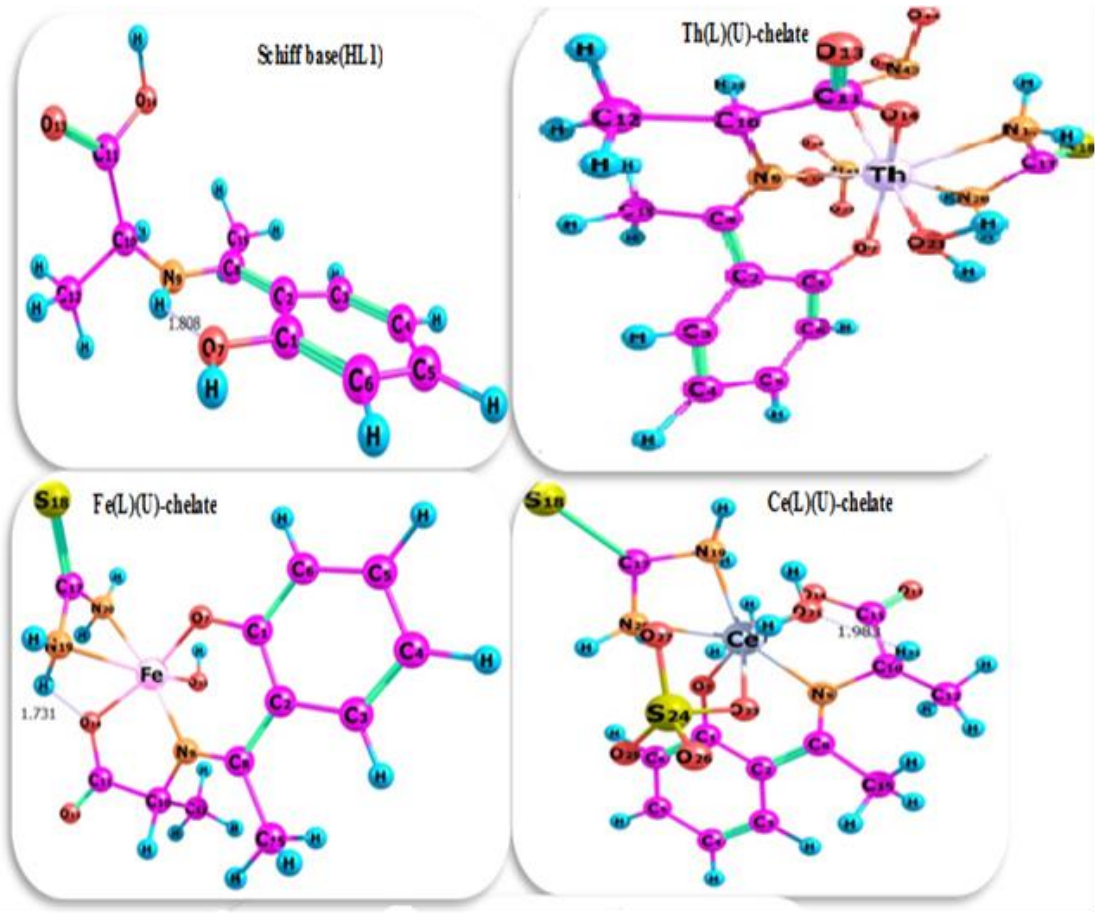

Fig. 5 Optimized geometry of Schiff base(HL) and mixed ligand chelates

The charges were changed to 0.384 in Fe(L)(U)-chelate, -0.138) in Ce(L1)(L2)-chelate and 0.043 in Th(L1)(L2)-chelate. All the mixed ligand chelates except Fe(L1)(L2)-chelate exhibits high values of dipole moment, which may favor their interactions with high dipole moment species (dipole-dipole interactions), especially in biological systems. HOMO energy (EHOMO) and LUMO energy (ELUMO) are often used as indices of reactivity of a molecule with respect to its readiness to donate and accept electron(s) respectively under favorable conditions. Table 5 shows the results of the equations for dipole moment(D), hardness(η), Softness(σ) Chemical potential(μ) and Electronegativity (x) which are calculated by the following equations:

$\eta = (I-A)/2$ $S = 1/2\eta$ $\mu = -(I+A)/2$ $x = (I+A)$ $I = -E_{HOMO}$ $A = -E_{LUMO}$

Where, I = the ionization potentialof the molecule
A =electron affinity of the molecule

The EHOMO and ELUMO are all negative, representative that the products are stable. All the metal complexes especially the chelate have low values of energy gap (ΔE) suggesting high reactivity and soft molecules. The order of softness is Th(L1)(L2)-chelate > Ce(L1)(L2)-chelate > ligand >Fe(L1)(L2)-chelate. Electron density distributions of the frontier molecular orbitals (FMOs), viz the highest occupied molecular orbitals (HOMOs) and lowest unoccupied molecular orbitals (LUMOs) are shown in Fig.13.The HOMO electron density of (HL1) is mainly distributed mainly over the aromatic ring but in case of its metal chelates the HOMO electron density distribution is extended to the whole ligand (HL1) atoms and the metal ions. Thiourea ligands not involved in the HOMO electron density distribution in iron chelate but Ce and Th chelates, all coordinated ligands involved in the electron density distribution. HOMO electron density distribution is extended to hydroxy group in Fe chelate. LUMO electron density of (HL) is distributed over the methyl and carboxylic acid groups. LUMO electron density of all chelates on the other hand is well distributed over nearly the entire atoms of all coordinated types of ligands and the central metal ions except Th(L1)(L2)-chelate, (HL1) ligand was partially involved in its electron density distribution. The generalization in iron chelates such that the thiourea unit is not significantly involved in the

HOMO electron density distributions. The implication of this is that the studied mixed ligand chelates will preferably interact with electrophilic species through the (HL1), OH and water units of the ligands. But in Ce and Th mixed ligand chelates, all ligands will preferably interact with electrophilic species through the (HL1), L2, SO_4, NO_3 and water units.

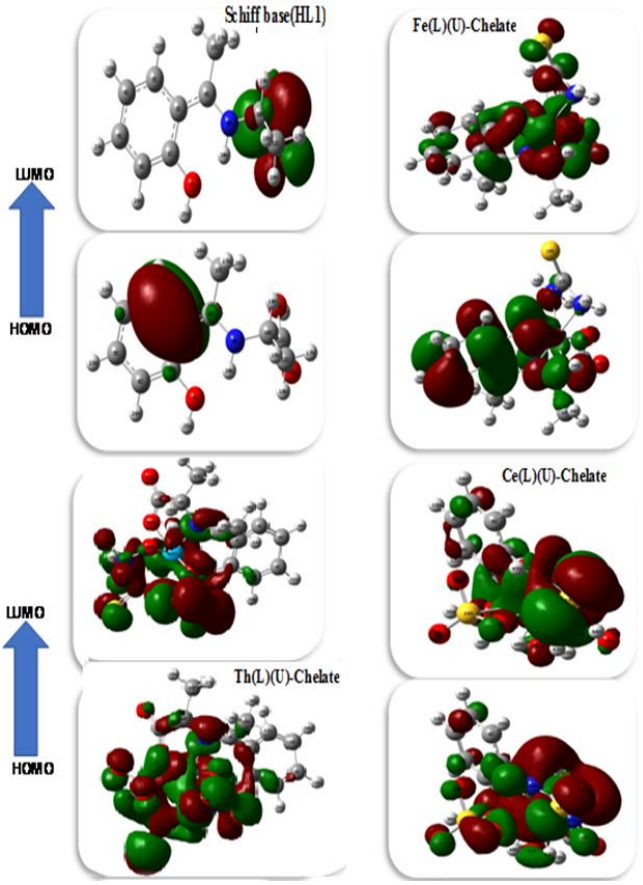

Fig 6: Molecular graphs of Schiff base(HL1) and mixed ligand chelates

Table 4: Some of the optimized bond lengths, Å and bond angles, degrees, for Schiff base and mixed-ligand chelates using B3LYP/6-311G and B3LYP/LANL2DE, respectively.

Bond length (A°)	Schiff base (HL1)	Fe(L1)(L2)-chelate	Ce(L1)(L2)-chelate	Th(L1)(L2)-chelate
R(C1-C2)	1.43812	1.43764	1.34110	1.33709
R(C2-C8)	1.43222	1.47342	1.35050	1.30820
R (C1-O7)	1.41412	1.34449	1.25381	1.20003
R (C8-N9)	1.39149	1.32001	1.17488	1.16573
R (N9-C10)	1.46663	1.49881	1.36985	1.40073
R (C10-C11)	1.52486	1.54400	1.45228	1.43878
R (C11-O14)	1.38356	1.35365	1.23821	1.17943
R (C17-N19)	---	1.41078	1.38741	1.34977
R (C17-N20)	---	1.44383	1.37918	1.37119
R (C17-S18)	---	1.67270	1.94671	1.41895
R (O23-S24)	---	---	1.48240	---
R (M-O7)	---	1.84211	1.52843	1.98808
R (M-N9)	---	1.92834	1.95181	1.96550
R (M-O14)	---	1.94711	1.79642	1.79872
R (M-O21-(H_2O))	---	---	1.81030	1.94788
R (Ce-O22-(H_2O))	---	---	1.86456	---
R (Fe-O33OH)	---	1.82247	---	---

R (M-N19)	---	2.20730	2.08294	2.20675
R (M-N20)	---	2.12305	2.00360	2.05219
R (Ce-O23-(SO_4))	---	---	2.03251	---
R (Th-O22)	---	---	---	1.88990
bond angles (degrees)				
Â(O7-C1-C2)	117.906	124.567	124.064	124.062
Â(C1-C2-C8)	124.730	123.538	115.534	117.413
Â(C2-C8-N9)	120.552	122.478	120.813	127.746
Â(C8-N9-C10)	126.586	122.846	120.436	129.520
Â(N9-C10-C11)	108.278	110.166	104.250	103.514
Â(C10-C11-O14)	111.579	114.252	112.037	106.953
Â(N19-C17-N20)	---	107.448	103.258	101.727
Â(N9-M-O7)	---	96.470	82.722	89.634
Â(N19-M-N20)	---	64.174	64.081	59.280
Â(O33-M-N9)	---	87.451	---	---
Â(Th-O22-N42)	---	---	---	110.167

Table 5: Ground state properties of Schiff base and some mixed ligand chelate using B3LYP/6-311G and B3LYP/LANL2DZ, respectively.

Parameter	**Schiff base (HL1)**	**Fe(L1)(L2)- chelate**	**Ce(L1)(L2)-chelate**	**Th(L1)(L2)-chelate**
E_T, Hartree	-1045.39976321	-1065.59006303	-8168.11829208	-18697.24970970
E_{HOMO}, eV	-4.64634638	-6.0145355	-4.48933661	-4.94022949
E_{LUMO}, eV	-2.41038572	-2.4209982	-3.29230717	-4.03109665
ΔE, eV	2.23596066	3.593537	1.197029	0.90913284
I=- E_{HOMO}, eV	4.64634638	6.014536	4.48933661	4.940229
A= - E_{LUMO}, eV	2.41038572	2.420998	3.29230717	4.031097
χ, eV	3.156018004	2.347417842	6.500795653	9.868003602
η, eV	1.11798033	1.796768675	0.59851472	0.45456642
S, eV^{-1}	0.44723506	0.278277336	0.835401342	1.099949266
μ, eV	-3.52836605	-4.217766845	-3.89082189	-4.48566307
Dipole Moment (Debye)	10.5480	3.8968	9.9783	13.9064

Anticancer activity

The in vitro growth inhibitory activity of the prepared Schiff base and its mixed ligand chelates (Th, Ce & Fe) on human liver cancer cell line, HepG2 was ascertained by exposing cells for to the medium with varying concentrations of compound (0–1000 μg mL^{-1}). All results were compared to the Doxorubicin standard drug. The results can be seen in (Fig. 7). After incubation with chelates a decrease in cell proliferation observed. The analysis of the obtained IC50 values reveal that the cerium (IV) chelates exerted superior activity in comparison to the iron and thorium compounds, the latter being the least active. The activity of the ligand is enhanced upon chelate-formation in case of Ce(IV) chelate. The higher conjugation in the ligand skeleton as a result of chelation process may be the reason for increased activity upon chelate formation [34]. The obtained results are consistent with the previously published work of metal chelates which were tested in vitro for their antitumor activities against Hep G-2 cell line [35]. The high activity of Ce(IV)-chelate may be due to its interaction more strongly with DNA than the ligand itself, with intercalation the most probable binding mode; and trigging DNA damage in hepatocellular carcinoma HepG2 cells, resulting in S phase cell cycle arrest and apoptosis as in the case of lanthanide complexes [36]. Also, the improvement of cytotoxic potency may be attributed to the positive charge of the metal increasing the acidity of coordinated ligand that bears protons, causing stronger hydrogen bonds which enhance the biological activity.

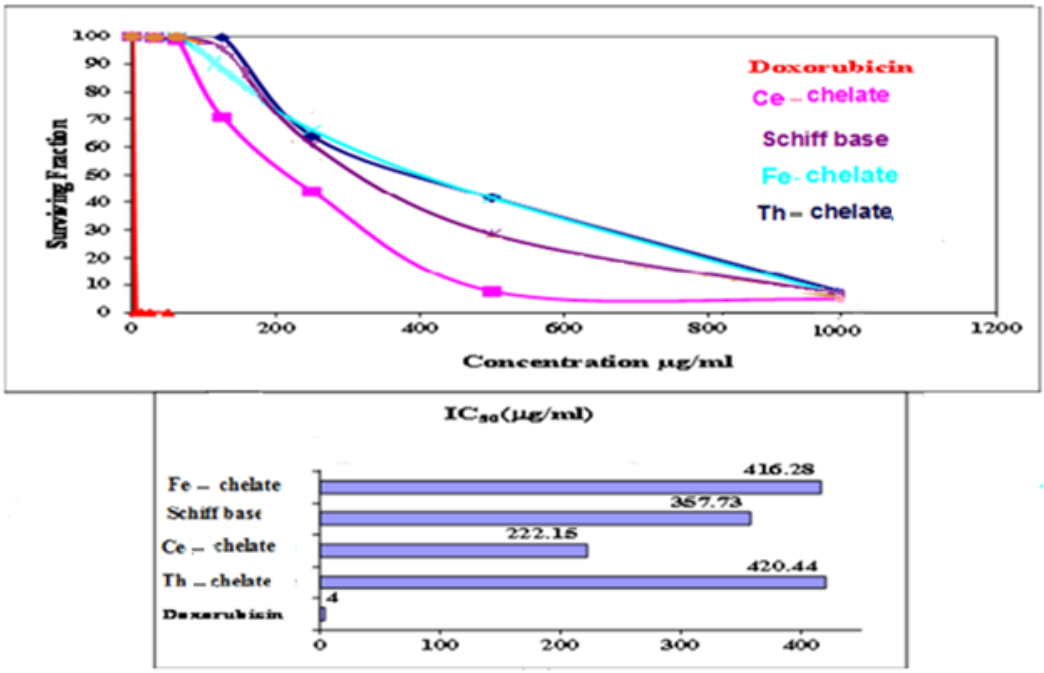

Fig.7: The surviving fraction of compounds against HepG2 liver cell

Table 6: Binding affinity of Schiff base and iron mixed ligand chelate against EGFR tyrosine kinase receptor (PDB Code: 1M17)

Antitumor docking 1M17			
Compound	**Scoring energy** (RMSD)	**Involved amino acids**	**Type of interaction**
Schiff base	-4.10(2.36)	---	Solvent contact
Fe-L1L2 chelate	-6.72(2.2)	Thr-830 and Lys-721	Side chain acceptor and side chain donor

Molecular docking studies

The molecular docking in this study for the ligand and iron(III) mixed ligand chelate as representative examples to compare their results with the experimental IC_{50} values. The scoring energy and root-mean-square deviation values are represented in (Table 6). Theoretically, the solvent contact of ligand show decrease in scoring energy values and consequence it was expected to give a decrease in its true experimental cytotoxic result. But the experimental results as discussed before revealed lower IC_{50} for ligand than Fe-chelate. Side chain acceptor and side chain donor interaction types were observed with Thr-830 and Lys-721 respectively through molecular docking of Fe-chelate.

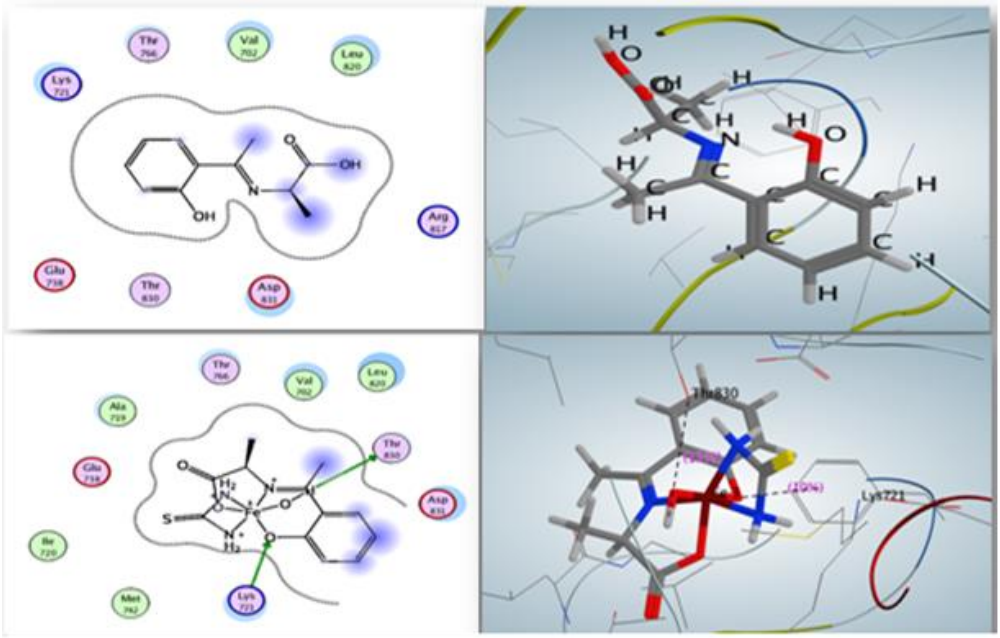

Fig. 8: 2D and 3D Binding affinity of Schiff base and iron-mixed ligand chelate against EGFR tyrosine kinase receptor (PDB Code: 1M17), respectively.

Conclusion

In this study, three mixed-ligand chelates of Fe(III), Ce(IV), and Th(IV) ions with a Schiff base derived from the condensation of L-alanine and o-hydroxyacetophenone (HL1) and thiourea as a secondary ligand (L2) were successfully synthesized and characterized by various physicochemical and spectroscopic techniques. The analytical data confirmed the formation of chelates with a 1:1:1 stoichiometric ratio (M:L1:L2) and a non-electrolytic nature. The magnetic susceptibility measurements revealed the paramagnetic behavior of the Fe(III) chelate and diamagnetic characteristics for Ce(IV) and Th(IV) chelates, suggesting octahedral geometries around the metal centers. Spectroscopic analyses, including IR, UV–Vis, NMR, and mass spectra, supported the proposed coordination through azomethine nitrogen, phenolic, and carboxylic oxygen atoms of the Schiff base, in addition to sulfur and nitrogen atoms from thiourea. The observed shifts and new absorption bands in the infrared and electronic spectra confirmed the successful metal-ligand interaction. Theoretical investigations using DFT (B3LYP/6-31G(d,p)/LANL2DZ) further validated the coordination pattern and provided insights into electronic properties, revealing that the Ce(IV) and Th(IV) chelates exhibited smaller HOMO–LUMO gaps, indicating higher reactivity and chemical softness compared to the Fe(III) chelate. The optimized geometries and charge distributions demonstrated the significant role of O and N donor atoms in complex stabilization. The synthesized chelates showed remarkable anticancer potential against the human hepatocellular carcinoma (HEPG-2) cell line, exhibiting pronounced cytotoxic activity. Molecular docking simulations against the EGFR tyrosine kinase receptor (PDB ID: 1M17) revealed favorable binding affinities and strong interactions with key amino acid residues within the receptor's active site, suggesting a plausible mechanism of anticancer action. Overall, the combined experimental and theoretical results highlight the successful design of Schiff base–thiourea mixed-ligand chelates with promising biological activity and well-defined structural, electronic, and binding properties. These findings suggest that such coordination frameworks could serve as valuable leads for the development of novel metal-based anticancer agents.

Acknowledgement

The authors would like to express their sincere gratitude to the University of Benghazi, Libya, for providing the necessary facilities, laboratory support, and research environment that made this work possible.

ETHICS

Not applicable.

Conflicts of Interest

The authors declare no conflicts of interest.

Author contributions: B.M.A. carried out the synthesis and spectral characterization of the ligands and metal complexes. M.M.E. supervised the work, contributed to data interpretation, and revised the final version of-

Funding: Not applicable.

References

1. Abduljalil, N., et al., Synthesis, Characterization, Antimicrobial Activity, DFT, Molecular Docking, and ADMET of 4-Chlorophenyazolquniolin-8-ol and Its Metal Complexes. AlQalam Journal of Medical and Applied Sciences, 2024: p. 566-582.

2. Bufarwa, S.M., et al., Antituberculosis, antimicrobial, antioxidant, cytotoxicity and anti-inflammatory activity of Schiff base derived from 2, 3-diaminophenazine moiety and its metal (II) complexes: structural elucidation, computational aspects, and biological evaluation. Reviews in Inorganic Chemistry, 2025. 45(1): p. 105-124.

3. El-Ajaily, M., N. Al-Barki, and A. Maihub, Mixed schiff base chelates: synthesis ans spectroscopic investigation. Asian Journal Advanced Basic Science, 2016. 4: p. 123-130.

4. El-Ajaily, M., et al., Schiff base derived from phenylenediamine and salicylaldehyde as precursor techniques in coordination chemistry. J Chem Pharm Res, 2013. 5(12): p. 933-938.

5. Binhamad, H.A., et al., Synthesis, Characterization (IR, Elemental analysis, Molar Conductivity), and Antibacterial Investigation of Complex produced by the reaction between Co (II) ion with mixed ligands of (Amoxicillin and Salen). Al-Mukhtar J. Basic Sci, 2023. 21: p. 98-104.

6. El-Barasi, N., et al., Synthesis, characterization, theoretical study and biological evaluation of Schiff base and their La (III), Ce (IV) and UO2 (II) complexes. Bulletin of the Chemical Society of Ethiopia, 2023. 37(2): p. 335-346.

7. Mohapatra, R., et al., E-Zahan, MK (2019). Recent advances in urea-and thiourea-based metal complexes: biological, sensor, optical, and corroson inhibition studies. Comments on Inorganic Chemistry. 39(3): p. 127-187.

8. El-Ajaily, M., S. Ben-Gweirif, and A. Maihub, &El-. tajoury, AN (2005), chelation behavior and biological activity of divalent metal ions towards Schiff-base derived from salicylaldehyde and histidine. Science and it's Application Journal. 1: p. 196-210.

9. Maihub, A., et al., Synthesis of Some Mixed Ligand Complexes Derived From Catechol And 2-Aminopyridine And Their Biological Activity. Journal of basic and applied Sciences, 2005. 15(1): p. 41.

10. Bufarwa, S., et al., Synthesis, characterization, thermal, theoretical studies, antimicrobial, antioxidant activity, superoxide dismutase-like activity and catalase mimetics of metal (II) complexes derived from sugar and Schiff base. Reviews in Inorganic Chemistry, 2024. 44(4): p. 521-533.

11. Bufarwa, S., S. Abdel-Latif, and H.B. Bahnasy, Spectroscopic, Thermal, and Conductometric Studies of Some (Arylazo) Quinolin-8-Ol and Their Complexes with the Divalent Ions of Mn, Ni, Cu, and Zn. Eur. Chem. Bull, 2023. 12: p. 187-197.

12. Amin, A., et al., In silico identification of a prognostic gene signature and virtual screening for hepatocellular carcinoma. Computational Biology and Chemistry, 2025: p. 108718.

13. Hasan, H., et al., Dieckol from Brown Algae Targeting the Hepatocellular Carcinoma Pathway: A Computational Pharmacology Study. Pharmacological Research-Reports, 2025: p. 100064.

14. Bibi, S., et al., Cordycepin and its structural derivatives effectively suppress the high expression of epidermal growth factor receptor (EGFR) tyrosine kinase in breast carcinomas: a computational drug development approach. Current Medicinal Chemistry, 2025. 32(26): p. 5582-5610.

15. Mohapatra, R.K., et al., DFT, anticancer, antioxidant and molecular docking investigations of some ternary Ni (II) complexes with 2-[(E)-[4-(dimethylamino) phenyl] methyleneamino] phenol. Chemical Papers, 2021. 75(3): p. 1005-1019.

16. Ali, F., et al., Pharmacophore-Based Discovery of Licoisoflavanone as a Dual CXCR4/CXCR7 Inhibitor for Coronary Artery Disease: Integration of Traditional Chinese Medicine and Modern Computational Approaches. Journal of Computational Biophysics and Chemistry, 2025.

17. Mustapha, B., et al., Computational approach: 3D-QSAR, molecular docking, molecular dynamics simulation investigations, drug-like-ness, and DFT score evaluation of a potential novel and retrosynthesis of some TR-H derivatives as Streptococcus pneumoniae drug. Karbala International Journal of Modern Science, 2025. 11(2): p. 9.

18. Maihub, A. and M. El-Ajaily, Synthesis Characterization and Biological Applications of Schiff Base Complexes Containing Acetophenone or Resemblance Compounds. Academic Journal of Chemistry, 2018. 3(6): p. 46-59.

19. Maihub, A., M. El-Ajaily, and S. Hudere, Synthesis and spectral studies of some transition metal complexes of Schiff base. Asian Journal of Chemistry, 2007. 19(1): p. 1.

20. Bufarwa, S.M., et al. Evaluation of Some Heavy Metals (Co, Zn, Pb, and Cd) in Sardines Cans Samples Taken from Some Markets in El-Beida City-Libya. in Libyan Journal of Basic Sciences (LJBS), Special Issue for 5th International Conference for Basic Sciences and Their Applications (5th ICBSTA). 2022.

21. Morad, F., M. Elajaily, and S. Ben Gweirif, Preparation, physical characterization and antibacterial activity of Ni (II) Schiff base complex. Journal of Science and Its Applications, 2007. 1(1): p. 72-78.

22. Morad, F., M. El-Ajaily, and A. Maihub, Preparation, characterization and antibacterial activity of some metal ion complexes. Egypt J. Anal. Chem, 2006. 15: p. 98-103.

23. Maihub, A., M. El-ajaily, and N. El-Hassy, Titanium (IV), Chromium (III) and Iron (III) complexes of Schiff base derived from aldehyde and primary amine. International Journal of ChemTech Research, 2012. 4: p. 631-633.

24. Saleh, M., et al., Algal Bioremediation: Heavy Metals Removal And Evaluation Of Biological Activities In Sewage Plant. Journal of Survey in Fisheries Sciences, 2023: p. 1355-65.

25. Saeed, S., et al., Utilizing Microbiological Techniques: The Residual Microorganisms in Poultry Flesh Raised at Random Between 2024 and 2025. AlQalam Journal of Medical and Applied Sciences, 2025: p. 958-960.

26. Abbass, L.M., et al., Exploring the anti-colon cancer potential of febuxostat-based mixed metal complexes with 2, 2′ -bipyridine: MTT assay, toxicity evaluation, prediction profiles, and computational studies. Inorganic Chemistry Communications, 2025. 178: p. 114460.

27. Hamil, A., et al., Synthesis of a New Schiff Base: 2-[2-(E)-(2-hydroxyphenyl)-ethylidene] aminoethyl) ethanimidoyl] phen. International Journal of ChemTech Research, 2012. 4(2): p. 682-685.

28. Mohapatra, R.K., et al., biological aspects of Schiff base–metal complexes derived from benzaldehydes: an overview. Journal of the Iranian Chemical Society, 2018. 15(10): p. 2193-2227.

29. Mohapatra, R.K., et al., Synthesis, spectral, thermal, kinetic and antibacterial studies of transition metal complexes with benzimidazolyl-2-hydrazones of o-hydroxyacetophenone, o-hydroxybenzophenone and o-vanillin. Bulletin of the Chemical Society of Ethiopia, 2018. 32(3): p. 437-450.

30. El-ajaily, M., et al., Experimental studies of azo Schiff base chelates and their corrosion inhibition behavior. Asian J. Adv. Basic Sci, 2014. 2(2): p. 17-30.

31. El-Ajaily, M., et al., Mixed-Ligand Chelate Formation of Co (II), Ni (II), Cu (II) and Zn (II) Ions with Schiff Base as Main Ligand and Amino Acid as Co-Ligand. International Research Journal of Pure and Applied Chemistry, 2015. 5(3): p. 229.

32. Hamil, A.M. and M.M. El-Ajaily, Synthesis and Physiochemical Investigation of Cobalt (II) and Nickel (II) Complexes of 1-2-[(Z)-2-(3-acetyl-4-hydroxyphenyl)-1-diazenyl] phenyl-1-ethanone. Journal of the Chemical Society of Pakistan, 2011. 33(6): p. 652.

33. Elajaily, M.M., et al., Synthesis, characterization and corrosion inhibition of cobalt (II) azo schiff base chelate. J Chem Pharm Res, 2013. 5(12): p. 1144-1151.

34. El-Ajaily, M., et al., Complex Formation of TiO (IV), Cr (III) and Pb (II) ions Using 1, 3-bis (2-hydroxybenzylidene) Thiourea as Ligand. Egyptian Journal of Analytical Chemistry, 2011. 20(16): p. 18-25.

35. Al-Resayes, S.I., et al., Synthesis, characterization, biological applications, and molecular docking studies of amino-phenol-derived mixed-ligand complexes with Fe (III), Cr (III), and La (III) ions. Journal of Saudi Chemical Society, 2023. 27(3).

36. Miloud, M., et al., Antifungal activity of some mixed ligand complexes incorporating Schiff bases. J Bacteriol Mycol, 2020. 7(1): p. 1122.

37. El-Barasi, N.M., et al., Synthesis, structural investigations and antimicrobial studies of hydrazone based ternary complexes with Cr (III), Fe (III) and La (III) ions. Journal of Saudi Chemical Society, 2020. 24(6): p. 492-503.

38. Mustapha, B., Synthèse et caractérisation de complexes de Zn (II), Hg (II) et Pb (II) avec quelques dérivés du 1, 2, 3-Triazole. 2007.

39. El-ajaily, M.M., et al., Transition Metal Complexes of (E)-2 ((2-hydroxybenzylidene) amino-3-mercaptopropanoic acid: XRD, Anticancer, Molecular modeling and Molecular Docking Studies. ChemistrySelect, 2019. 4(34): p. 9999-10005.

40. Bufarwa, S. and S. Abdel-Latif, Spectroscopic, thermal, and conductometric investigation of some (arylazo) quinolin-8-ol and their complexes with the divalent ions of Mn, Ni, Cu, and Zn. 2022.

41. BELAIDI, M., et al., Integrated 3D-QSAR, Molecular Docking, Molecular Dynamics Simulation, ADMET, Drug-Likeness, and DFT Score Evaluation of a Potential Novel 1, 2, 3-Triazole-Hybrid Streptococcus Pneumoniae Drug. Molecular Docking, Molecular Dynamics Simulation, ADMET, Drug-Likeness, and DFT Score Evaluation of a Potential Novel. 1(2).

42. Mustapha, B., et al., Exploring the Antituberculosis, Anti-Inflammatory, and Antimicrobial Activities and Computational Potential of Quinoline-8-ol Azo Dye Complexes. Applied Organometallic Chemistry, 2025. 39(8): p. e70310.